Tutor
Dra. Esther Santamaría Hernández
Departament d'Enginyeria Química

Grau en Enginyeria Química

Treball Final de Grau

Use of ion exchange column to obtain ordered mesoporous materials.

Ús d'una columna de bescanvi iònic per l'obtenció de materials mesoporosos ordenats.

Cristian Méndez Lisón

June 2015

Universitat de Barcelona

Dos campus d'excel·lència internacional
B:KC Barcelona Knowledge Campus
HUBc Health Universitat de Barcelona Campus

The engineer's art is the art of the possible.

Santiago Calatrava

Para empezar quiero dar las gracias a Esther Santamaría no solo por su apoyo y su manera de llevar un trabajo final de carrera sino también por transmitirme sus conocimientos así como sus ganas por descubrir más.

También agradecer a toda la gente que me ha apoyado en estos 4 años de carrera: mi familia, mi pareja; mis ex compañeros de instituto, mis amigos de toda la vida y como no… mis compañeros de batallas en estos 4 años: mis compañeros de universidad. Gracias a todos ellos, por ayudarme en las adversidades encontradas y facilitarme aún más los buenos momentos.

Desde que entré en primer curso hasta poder graduarme he vivido muchas experiencias que me han formado como persona y me han llevado a ser tal como soy y por ello es de agradecer el esfuerzo y dedicación de cada una de las personas de los distintos departamentos de la Facultad de Química de la UB, en especial al departamento de Ingeniería Química.

¡Gracias!

REPORT

CONTENTS

1. SUMMARY

In fields such as medicine, diagnostic applications... or operations such as catalysis, chromatographs, the adsorption of gases and liquids... materials with large values of specific surfaces are required because surface phenomena are involved in operations. Recently, mesoporous materials have been studied with the aim of having the highest possible surface area.

Mesporous materials have pore diameter between 20 and 50 Å, with high values of specific surfaces. The order of the pores in space influences the value of the specific surface obtained. When porous are ordered in the space the surface area is greater than when the porous are disordered. In order to maximize the value of the specific surface, it is desirable to obtain ordered mesoporous materials.

It is possible to obtain different properties of silica materials with small variations in the processes of its synthesis in these materials. This is why the synthesis of mesoporous materials is studied with the aim of have them ordered such as getting (or not) mesoporous materials.

Nowadays, the TEOS or TMOS silica sources are used in obtaining mesostructured silicas. These sources of silica are intended to be replaced by substitutes and the use of sodium silicate as an alternative source of silica may have greater advantages on an industrial scale because, among other reasons, it is cheaper than TEOS or TMOS.

It also aims to obtain an alternative process of silica synthesis mesoporous materials because nowadays acid catalysts are used as a proton source involving a washing process which can be avoided by using ion exchange resins as proton source.

Therefore, the use of sodium silicate as well as the use of ion exchange resins in columns provides greater benefits from the industrial punt of view.

This is why this project is based chiefly on the synthesis of mesoporous material using a column with ion exchange resin. The variables studied are the relations of surfactant: water and

the ratio of sodium silicate: water. They are chosen from previous studies in the synthesis of mesoporous materials. The variable to maximize is the surface area of the materials obtained.

Ion exchange column should be studied because working ranges must be known in order to obtain desired mesoporous materials. The first step is to obtained ion exchange resin column rupture curves.

Microscopy techniques such as TEM and SEM and other techniques as BET and SAXS are used in order to characterize the synthesized mesoporous silica materials from the ion exchange column.

The results obtained are subjected to statistical analysis using the "Statgraphics Plus 4.1" program having Pareto charts and estimated response surfaces.

The last step is to study the influence of the ratio of surfactant:water and sodium silicate:water in the studied range. It has been found that the ratio of sodium silicate:water a maximum value of the obtained specific surface is obtained corresponding with the maximum management of these materials. In the range studied, the ratio of surfactant:water has not been a significant variable in the value of specific surface area of the materials obtained.

Keywords: mesoporous materials, silica, ion exchange column.

2. RESUMEN

En ámbitos como la medicina, las aplicaciones de diagnóstico… o en las operaciones como la catálisis, las cromatografías, las adsorciones de gases y líquidos… se requieren materiales con grandes valores de superficies específicas puesto que, en dichas operaciones, se ven involucrados fenómenos de superficie. En los últimos años los materiales mesoporosos han sido objeto de estudio con el fin de que posean una superficie específica lo más alta posible.

Los materiales mesporosos son aquellos materiales con diámetro de poros comprendidos entre 20 y 50Å, con elevados valores de superficies específicas. El orden de los poros en el espacio influye en el valor de la superficie específica obtenida. La disposición que maximiza la superficie específica es la de poros ordenados en el espacio mientras que si se obtiene una disposición al azar se minimiza. Con el objetivo de maximizar el valor de la superficie específica, por tanto, es conveniente la obtención de materiales mesoporosos ordenados.

Con pequeñas variaciones en los procesos de síntesis de los materiales de sílica se pueden obtener distintas propiedades en dichos materiales así como llegar a obtener o no materiales mesoporosos ordenados.

Hoy en día el TEOS o el TMOS son las fuentes de sílice utilizadas en la obtención de sílicas mesoestructuradas. Dichas fuentes de sílice pretenden ser reemplazadas por otras alternativas y el uso de silicato de sodio como fuente alternativa de sílice puede presentar mayores ventajas a escala industrial ya que, entre otras razones, es una fuente de sílice más económica que el TEOS o TMOS.

También se pretende obtener un proceso alternativo de síntesis de los materiales mesoporosos de sílica ya que actualmente se trabaja con catalizadores ácidos como fuente de protones implicando un proceso de lavado que puede ser evitado usando resinas de intercambio iónico como fuente de protones.

Por tanto el uso de silicato de sodio así como el uso de resinas de intercambio iónico en columnas proporcionan mayores beneficios desde el punto de vista industrial.

Por todo ello, el estudio de este trabajo se basa principalmente en la síntesis de material mesoporoso mediante el uso de una columna con resina de intercambio iónico. Las variables de estudio son las relaciones de tensioactivo:agua y de silicato de sodio:agua. Las variables de estudio son escogidas a partir trabajos previos en la síntesis de materiales mesoporosos. La variable a maximizar es la superfície específica de los materiales obtenidos.

Es preciso caracterizar la columna de intercambio iónico puesto que se debe conocer en que rangos se debe de trabajar con el fin de obtener los materiales mesoporosos deseados. Para la caracterización de la columna de intercambio iónico se deben obtener las curvas de ruptura.

La caracterización de los materiales mesoporosos de sílica sintetizados a partir de la columna de intercambio iónico se realiza mediante el uso de técnicas de microscopía como TEM y SEM así como de técnicas de caracterización como BET y SAXS.

Los resultados obtenidos se someten a un análisis estadístico con la ayuda del programa "*Statgraphics Plus 4.1*" obteniendo gráficos de Pareto y superficies de respuestas estimadas.

Con todo ello, finalmente se estudia la influencia de la relación de tensioactivo:agua y la influencia de silicato de sodio:agua en el rango estudiado. Se ha comprobado que para la relación de silicato de sodio:agua se obtiene un máximo en el valor de la superficie específica obtenida que corresponde con el máximo de ordenación de éstos materiales. En el rango estudiado, la relación de tensioactivo:agua no ha sido una variable significativa en el valor de la superficie específica de los materiales obtenidos.

Palabras clave: materiales mesoporosos, sílica, columna de intercambio iónico.

3. INTRODUCTION

3.1. MESOPOROUS MATERIALS

The porosity of a material can be defined as the extent of their empty spaces. Void spaces are known as pores that constitute the material.

The word “pore” comes from the Latin term “porus” and it turns from Greek πόρος (pores) which means step-passage. This definition can give us a clear idea of the role of a pore as a path between internal and external surface of a solid which allows the passage of vapours or gases.

Porous materials are classified according to IUPAC [1] depending on the size of pores:

Microporous Materials: Pore diameter less than 20 Å.

Mesoporous Materials: Pore diameter between 20 and 50 Å.

Macroporous Materials: Pore diameter greater than 50 Å.

Because of the mesopore structure, the advantages of mesoporous materials have been demonstrated [3]:

- Their structures can be highly ordered and size-controlled that allows the size-selective adsorption of small molecules and excludes the larger ones.
- They have high surface areas and large pore volumes that provide enough adsorption capacity.
- They have thermal and chemical stability, compositional controllability and flexibility in post-functionalization to allow the further introduction of hydrophilic, hydrophobic, polar and also positive and negative charged functional moieties on its surface.

3.2. BACKGROUND

Mesoporous materials were developed three decades ago [2]. The first material was a clay with rectangular pores [4]. The problem of that material was that reactives could not easily pass through it. Furthermore, pores had a wide size distribution and they were disordered in the space.

The meaning of "template" had not reached yet. In the early 90s, scientists from the company Mobil Corporation and Japanese scientists reported the synthesis of mesostructured silicates [4-5].

Zeolites are well-known members of the microporous class [6], which provide excellent catalytic properties by virtue of their crystalline aluminosilicate network. However, their applications are limited by the relatively small openings; therefore, pore enlargement was one of the main aspects in zeolite chemistry. Larger pores are present in porous glasses and porous gels, which were known as mesoporous materials at the time of the discovery of MCM-41 [6-7]. MCM-41, which stands for Mobil Composition of Matter number 41, shows a highly ordered hexagonal array of unidimensional pores with a very narrow pore size distribution. The walls, however, are very much resembling amorphous silica.

MCM-41 was discovered in the early 1990s [6-7]. This discovery has been a breakthrough in materials engineering and since then there has been impressive progress in the development of many new mesoporous solids based on templating mechanisms related to the one used for the original MCM-41 synthesis. Depending on the synthesis conditions, the silica source or the type of surfactant used many other mesoporous materials can be synthesized following the co-operative assembly pathway. In addition to the co-operative pathway, also exist the true liquid crystal templating pathway for obtaining mesoporous materials [8].

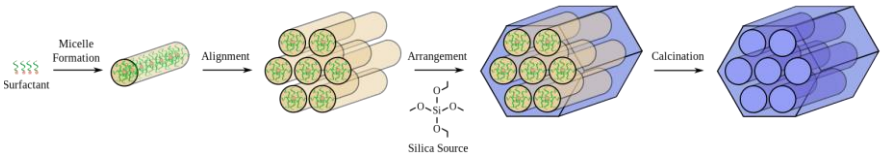

Figure 1. Synthesis pathway of MCM-41 [9].

3.3. MESOPOROUS SILICATE MATERIALS

Silica molecular sieves are the mesoporous materials most investigated because of previous studies about silicate sol-gel process [10]. Yanagisawa reported the first ordered mesoporous material in 1990 [11] and subsequently research by Mobil Oil Corporation generated MCM-41 and the M41S family of mesoporous silicates [12].

Thereafter, silica based mesoporous materials with different mesostructures have been synthesized usually using tetraethylorthosilicate (TEOS) as the hydrolysable silica building block, and long chain ammonium surfactants, amines or triblock copolymers as templating agents. Examples of these materials are MCM-41 (p6mm) [12], MCM-48 (Ia3d) [13], HMS and MSU (wormlike) [14], KIT-6 (Ia3d) [15], SBA-1 and SBA-6 (Pm3n) [16][17], SBA-2 and SBA-12 (P63/mmc),3 SBA-15 (p6mm) [18][19] and SBA-16 (Im3m) [18].

Moreover the mesoscale structure, other attemps have been done in controlling the materials in different morphologies by changing the process conditions.

. Various forms have been obtained, as it is shown in figure1. Some examples of these forms are thin films [20], fibers [21] monoliths [22], particles [23], and other interesting shapes [23].

Figure2. It shows a surfactant liquid crystal first solidified and then transformed into a mesoporous material by removal of the surfactant. Surfactant removal can be made either by washing or by calcinations [24].

Besides thin films, particles possessing mesopores of well-defined size and connectivity are of interest for catalysis, chromatography, controlled release, as fillers with low dielectric constant, and as hosts for optically active compounds [25].

3.3.1. Why silica?

1. Silica can be produced by sol–gel methods. The precursors used are not very reactive, despite other precursors for oxidic materials as titania, tin oxide, etc. This is why this process is easily controlled. Alkoxysilane compounds are used in most cases. The general process which is going on is given by the reaction scheme [26]:

$$Si(OR)_4 + H_2O \rightarrow [Si(OH)_4] \rightarrow SiO_2$$

Equation 1: General reaction of the silica

2. Free energy of silica is very close to its most stable form crystalline quartz. Furthermore, the Si-O bonds are so strong that the silica sol–gel process has highly irreversible character. Silica forms in its amorphous form and this amorphous silica is stable over a very high temperature range and period of time. All these statements demonstrate that the shape of silica can be formed at room temperature and then be retained a long time. Once more, this distinguishes silica from other materials where crystallization frequently leads to a restructuring in the network and therefore can destroy the mesostructure.

3. Finally, the interactions between surfactants or block copolymers can be tuned because silica units are available in anionic, neutral, or cationic form with dependence on the media pH. Further, the charge density on these silica precursors matches the charge density of the surfactant head groups quite well. Silica precursors and amphiphiles are compatible.

3.4. APPLICATIONS OF MESOPOROUS MATERIALS

The potential applications as supports for catalysis, separation, selective adsorption, novel functional materials and use as hosts to confine guest molecules due to their extremely high surface areas combined with large and uniform pore sizes is why silicate mesoporous materials have recieved widespread interest. A constant has been developed for larger pores with well-defined pore structures.

Here there are some applications:

Drug delivery systems

The main challenge in the development of drug delivery systems (DDS) is that drug efficacy diminishes before reaching the target, primarily due to the excretion of the drug from the body. [27].

In addition, the drug carrier must be non-toxic and inert during the treatment period. Because most biological molecules and pharmaceuticals are on the order of a few nanometers, nanoporous silica with a pore size of 2-30 nm is of great relevance for such life science applications.

Catalysis

In catalysis, high surface area materials with nanoscale features are used to develop highly selective catalysts that reduce energy use and waste/pollutant generation in industrial applications [28]. Porous materials, such as zeolites (microporous solids) are widely used in industry as catalysts and catalyst supports. However, when large molecules are involved in a catalyzed reaction, mass transfer limits the suitability of zeolite structures. Attempts to improve the diffusion of reactants to catalytic sites have been resolved by enlarging pore sizes to the meso range. These ultra-selective catalysts can cut costs significantly in many industries.

Diagnostics

Mesoporous materials are ideal in diagnostics applications due to their increased image contrast and chemical stability. [29] Moreover, functional moieties can be conjugated within the pores enables new possibilities for multiple measurements and detection. Due to the low toxicity of silica baser porous materials and their ability to host a variety of fluorescent markers, dyes and drugs can be used to track the location of therapeutic agents and their activity.

Adsorbents

The high surface area of nanoporous materials allows their use as adsorbents for various gases, liquids and toxic heavy metals. The uptake of these substances can be increased signicantly based on the surface properties (hydrophobicity, hydroplilicity, or functionality), of these mesoporous materials. Several applications, such as removal of pollutants from water, storage of gases (CO_2, H_2, CH_4, H_2S), [29-30] adsorptive xylene separation and separation of biological and pharmaceutical compounds have been addressed through the use of mesoporous materials as adsorbents.

Chromatography

The large pore volume, surface area and narrow pore-size distribution of mesoporous silica, makes it a good candidate for size exclusion chromatography. [31] These materials have been proposed as supports or stationary phases for size exclusion chromatography [32], capillary gas chromatography [33], proteomics separations, normal phase a High Pressure Liquid Chromatography (HPLC), as well as enantioselective HPLC.

3.5. FORMATION MECHANISMS OF MESOPOROUS MATERIALS

Mesoporous materials are synthesized by adding surfactant. For this reason, the concentration of the surfactant is different in each type of synthesis. The CSA synthesis uses a smaller concentration of surfactant than the LCT synthesis. Both syntheses have in common the formation of a liquid crystal. Finally, the surfactant is calcined or removed.

Formation of MCM-41 was through a liquid crystal formation synthesis. This could be via a LCT pathway or a CSA pathway (Figure 3).

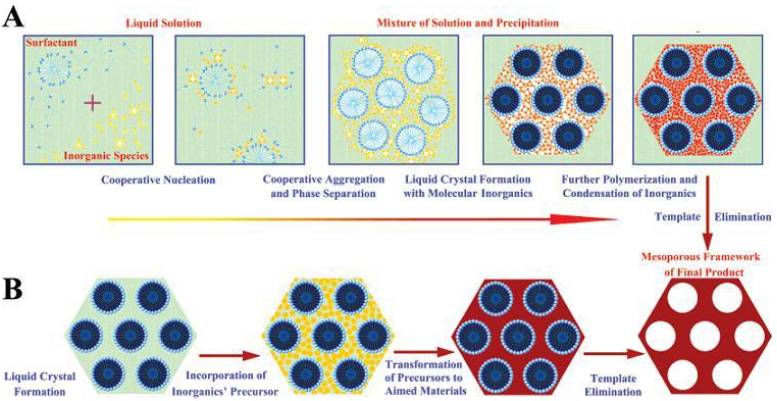

Figure 3. Synthetic Pathway: (A) CSA process (B) LCT process. [34].

3.5.1. LCT (Liquid Crystal Template proces)

Precursor interacts with a liquid crystal. Liquid crystal is synthesized without using precursor cooperation. Surfactant is put on an air-water interphase solution where micelles are formed and after concentration is raised (it can go from 25 to 40 surfactant percents) liquid crystals are formed. Precursor is added after liquid crystals are formed and it condenses in the hydrophilic domain of these crystals so when organic part is removed (template) only precursor is left and inorganic part becomes the ordered porous structure.

3.5.2. CSA (Cooperative Self-Assembly)

Surfactant and precursor cooperate to form the final structure. The surfactants are amphiphilic so the hydrophilic head interacts with the inorganic species in solution to form the composites. Surfactant begins to arrange in micelles when critical micellar concentration is raised. Then precursor is added into the surfactant solution and is starts condensing around micelles and this micelles are arranged with surrounding micelles forming cylinders or rods and precursor condenses around forming and organic-inorganic hybrid structure. This way uses less surfactant than an LCT process. After forming the inorganic structure it is necessary to remove the surfactant by calcinations.

3.6. ION EXCHANGE

3.6.1. Theoretical basis

Ion exchange is a separation operation which consists in transfer of fluid-solid material [35]. It involves the transfer of one or more ions of the fluid phase to the solid by exchange or displacement of ions of the same charge attached by electrostatic forces to surface functional groups. The solid-fluid balance and mass transfer rate will determine the efficiency of the process.

Polymer solids based on synthetic resins are the most common. This ion exchange resin is considered a structure of hydrocarbon chains joined to free ionic groups which are linked together transversely forming a three dimensional matrix which provides rigidity to the resin. The degree of crosslinking determines the internal pore structure.

Ions must diffuse within the resin for the exchange to occur. The degree of crosslinking can limit the mobility of ions participants. Charges of immobile ionic groups are balanced with free

ionic groups counter ions. These counter ions exchanged with ions of the dissolved electrolyte. If they are cations, ion exchangers are known as cationics and when they are anions, anionic. Ion exchange can be explained as a reversible reaction involving chemically equivalent amounts.

3.6.2. Ionic exchange in fix bed

The ion exchange operation is typically performed semi-continuously in a fixed bed of resin where a solution flows through it. The operating regime is non-stationary because the ion concentration varies continuously at each point of the system. The installations are generally formed by two identical beds. Thus, in one bed the solution which contains ions to exchange flows through it and the other bed is being regenerated [36].

At the beginning of the operation of a bed, most of the mass transfer happens near the inlet where the fluid bed is contacted with cool exchanger. Over time, the solid next to the entrance is almost saturated and most of the mass transfer takes place far from the entrance. Due to the resistance of the system to transfer ions from the bulk liquid to clearinghouses, a concentration gradient in the bed is established (Figure 4).

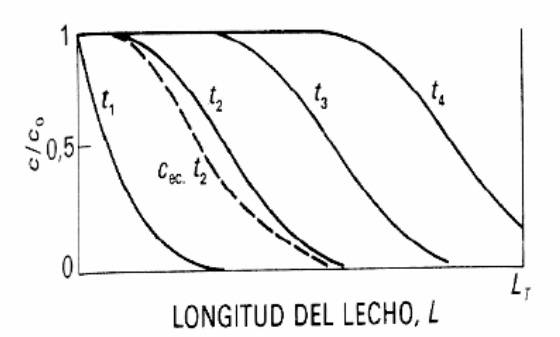

Figure 4. Concentration profiles in the bed over time [36].

The mass transfer zone is where most of the exchange of concentration takes place. This zone separates the unspoilt resin area from the saturation area. Boundaries are usually taken as c/co=0.95 a 0.05. As the ion exchange proceeds, the mass transfer zone in the bed moves to reach its lower end. Once it reaches the lower end, the outlet solution will contain increasing amounts of the exchange ions.

Break Time (TR) is the time from the beginning of the operation in the bed until the dissolution ions appear in the output current (where the maximum allowable concentration in the effluent reached) time [37]. At this time, the current is diverted to a second bed, beginning the process of regeneration of the first.

The breakthrough curve (Figure 5) represents the evolution of the concentration of the effluent leaving the bed. His knowledge is fundamental to design a fixed bed ion exchange. It must be determined experimentally given the difficulty of its prediction.

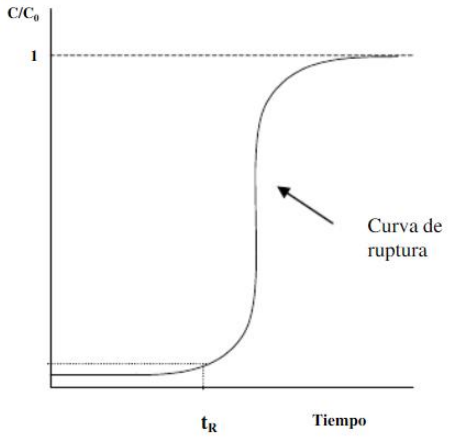

Figure 5. Diagram concentration – time [36].

3.6.3 Ion exchange Resins

The most important class of ion exchangers is the organic ion-exchange resins. They are typically gels. Their framework, the so-called matrix, consists of an irregular, macromolecular, three-dimensional network of hydrocarbon chains. The matrix carries ionic groups such as:

$$-SO_3^- \ , \qquad -COO^- \ , \qquad -PO_3^{2-} \ , \qquad -AsO_3^{2-}$$

in cation exchangers, and

$$-NH_3^+ \ , \qquad =NH_2^+ \ , \qquad \equiv N^+ \ , \qquad \equiv S^+$$

in anion exchangers. Ion-exchanger resins thus are crosslinked polyelectrolytes [38].

3.6.4. Why Ion Exchange?

Disadvantages of synthesis of mesoporous materials on an industrial scale

The main problem of the synthesis of mesoporous material in industry is to work in acidic medium. This means to work with acids to acidify and have a fairly acidic pH. The synthesis must be done batchwise due to the fact that working with acid pH and the need to was the material in order to remove the Na^+ cations does not accept a continuous operation, which also means an economic cost in the process.

So the problems are:

- Must work batchwise
- Use of acids.
- Final washing step: an economic cost

Advantages of using the ion exchange column

The main advantages of using the ion exchange column for obtaining ordered mesoporous material are in the industrial environment. Nowadays it is known that there are some new advantages which did not exist before:

- Working continuously: It is possible to have more than one column working while other columns are regenerating.

- Acid compounds are not required.

- Material washing step is avoided.

4. OBJECTIVES

Research of the synthesis of mesostructured materials is increasingly important because materials with a large surface area are required in various operations (such as catalysis, chromatography ...).The synthesis of mesoporous silica materials is made from a template surfactant where the mesoporous silica is obtained from a precursor source of silica.

In order to improve the synthesis at industrial level, it is intended to change the precursor silica sources that are currently used (TEOS and TMOS) for sodium silicate due to its advantages. It is also intended to change the currently synthesis using iong exchange column as an alternative. These two changes have great advantages in the synthesis on an industrial scale.

Therefore, the objectives are:

1) Obtaining ordered mesoporous silica materials using an ion exchange column as proton source and sodium silicate as the silica precursor.

2) Characterize the materials synthesized by microscopy techniques such as SEM and TEM and characterization techniques BET and SAXS.

3) Study the influence of surfactant:water ratio and sodium silicate:water on the value of the specific surface obtained from the synthesized mesoporous materials.

5. MATERIALS, EQUIPMENTS AND METHODS

5.1. MATERIALS

The materials used for the experiments were:

5.1.1. Liquid reactants

- 37% concentrated hydrochloric acid (HCl), Panreac.
- Sodium silicate solution (26.5% SiO_2 ~), Sigma Aldrich.
- Deionized water.

5.1.2. Solid reactants

- Pluronic P84. Poly (ethylene glycol) -poly (propylene glycol) -poly (ethylene glycol) (Sigma Aldrich).

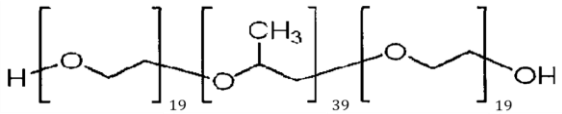

- Sodium hydroxide ≥ 98% as pellets, Sigma Aldrich.

5.1.3. Other materials

- Resin of ion exchange. Amberlyst 15, particle size ranging between 0.1-0.8 mm, Merck.

5.2. EQUIPMENT

The equipments used for the experiments were:

- Balance COBOS model AX 200 with capacity of 200 g and precision of 0.10 mg.
- Heater, PREBATEM model, J.P.Selecta.
- Stirrer, Eurostar model, IKA Werke (working range 0-2000 rpm).
- Muffle, HD-230 Obersel.
- Ion exchange column. (Column dimensions: height 23 cm and diameter 2.80 cm).
- Peristaltic pump, MCP Standard Ismatec. ISM 404.
- Transmission electron microscope (TEM). FEM-2100 Electron Microscope JEOL.
- Electron Microscope SEM. S-4100, Scanning Electron Microscope HITACHI.
- BET. Micromeritics Tristar 300.
- SAXS. Hecus X-ray Systems GMBH Graz.

5.3. METHODS

5.3.1. Experimental design

Experimental design, also called statistical design of experiments, is a methodology based on statistical and mathematical methods, where the aim is to help the experimenter to choose an optimal strategy while doing the minimum number of possible experiments to obtain the maximum information and assess results.

It can be applied in systems with one or more experimental variables. There are dependent variables (y) or other responses or controllable variables called independent factors (x). Such responses are also affected by uncontrollable variables (factors z).

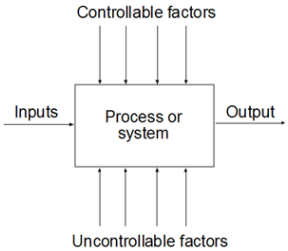

Figure 6. Experimental design representation.

5.3.2. Proposed experiments

Nine experiments were performed to test the influence of the ratio of surfactant, water and silicate. Working conditions were chosen based on a previous work: "*Study of the preparation of silica mesoporous materials by ion exchange resin*" by Jennifer Alegre Miranda:

-Working at a constant rate of 24,95mL / min

-Working with the same mass of resin for all experiments.

The mass ratio was varied in the experiments. The ratio of water was set at a value of 30 for all experiments and relations of sodium silicate solution and surfactant were changed. The ratio of silicate was changed at 1, 2 and 3 and surfactant ratio was changed at 0.25; 0.5 and 0.75. Finally experiments made were:

Chart 1. List of performed experiments.

	Mass ratio		
Experiment	Sodium silicate solution	Water	Surfactant
1	1	30	0.25
2	1	30	0.50
3	1	30	0.75
4	2	30	0.25
5	2	30	0.50
6	2	30	0.75
7	3	30	0.25
8	3	30	0.50
9	3	30	0.75

5.3.3. Mesoporous materials synthesized by ion exchange

For the synthesis of mesoporous materials from self-aggregation cooperative route (CSA), were made 9 experiments that were presented above. The aim was to check the influence of the composition variables on the material properties.

5.3.3.1. Obtaining the rupture curves

To perform the synthesis of mesoporous materials using ion exchange resin column it must be characterized, so rupture curve has to be known for the suitable values of work.

To obtain the rupture curve of the column it was decided to get 3 rupture curves for different ratios of sodium silicate:water used for obtaining mesoporous materials. The column operated flow was set at 24.95mL/min in the 3 cases in order to lock the variable. The flow rate was set in the aforementioned value obtained provided breakage curve at times greater than 5 minutes. Below are more detailed data of the solutions used for obtaining the rupture curves.

Chart 2. Data of the solutions used for obtaining the rupture curves.

	Mass ratio		**Mass [g]**	
Experiment	Sodium silicate solution	Water	Sodium silicate solution	Water
1	1	30	22.58	677.42
2	2	30	43.75	656.25
3	3	30	73	730

The experimental procedure for obtaining the rupture curves is explained below:

The installation was made by a column of ionic exchange with a height of 23 cm and 2.80 cm of diameter. The column had a height of about 10 cm resin (about half of the total column height). It was chosen in order to have enough amount of resin and ensure correct ion exchange. Furthermore, the installation had a peristaltic bomb in order to work in constant flow and a pH meter to make measurements over time pH.

In parallel, the solution sodium silicate and water was prepared. The initial pH of the solution was measured.

The solution was passed through the ion exchange column while maintaining the level of solution in the constant column so as to operate at a constant rate over time. pH measures over time in the lower outlet of the column is performed until the final pH reached a value of approximately 95% of the initial pH of the solution. Thus the data to characterize the breakthrough curves of the column according to the ratio of sodium silicate and water was obtained.

After the completion of each experiment the remains of sodium silicate were removed by dissolving NaOH and regenerating the column with protons. It was first washed with about 200 mL of deionized water and then with NaOH (1M) in order to dissolve any remaining silica. Then the resin was regenerated using 100 mL of a solution of HCl (2M) in order to obtain the H + column and finally the resin was washed with deionized water

Once the installation was prepared, the next step was to get the rupture curves.

First of all, protons were added to the resin placing it in a beaker and introducing 100 mL HCl (2M). Subsequently, the remaining HCl was removed with 200 mL of deionized water, introducing the protonated resin to the column.

At the same time, a sodium silicate and water solution was made with corresponding amounts and initial pH value of this solution with water was measured.

The following step was to pass the solution through the ion exchange column while maintaining the level of solution in the constant column to operate at a constant rate over time. pH measures over time in the lower outlet of the column were performed until the final pH reached a value of approximately 95% of the initial pH of the solution.

When each experiment was finished, the remains of sodium silicate were removed by dissolving NaOH and regenerating the column, (adding protons again). The next process was to remove the ion exchange resin column and transferred to a beaker. First, it was washed with 200 mL of deionized water and then with NaOH (1M) to dissolve any remaining silica. The resin was regenerated using 100 mL of a solution of HCl (2M) in order to obtain the H^+ column and finally the resin was washed with deionized water.

5.3.3.2. Synthesis of mesoporous materials

Once obtained the rupture curves of the ion exchange column, the experiments were performed with the aim of obtaining the materials mentioned above. With the rupture curve the maximum to operate in each case was determinated in order to have a lower 2.0 – 2.5 pH solution. Using this criterion, it was decidet that 1:30 silicate:water ratio had a 8.5min operation time, 2:30 ratio a 4.5min and 3:30 ratio a 3min time.The details of each experiment such as each mass values are shown below:

Chart 3. Mass details of experiments.

		Mass ratio			Mass [g]		
Experiment	**t operation [min]**	Sodium silicate solution	Water	Surfactant	Sodium silicate solution	Water	Surfactant
1	8.5	1	30	0.25	9.60	288.00	2.40
2	8.5	1	30	0.50	9.52	285.72	4.76
3	8.5	1	30	0.75	9.45	283.46	7.09
4	4.5	2	30	0.25	12.40	186.05	1.55
5	4.5	2	30	0.50	12.31	184.60	3.08
6	4.5	2	30	0.75	12.21	183.21	4.58
7	3	3	30	0.25	11.28	112.78	0.90
8	3	3	30	0.50	11.19	111.94	1.87
9	3	3	30	0.75	11.11	111.11	2.78

The experiments were conducted using the following methodology:

First of all, the grams of the sodium silicate solution, water and surfactant were weighed for the experiment.

The sodium silicate solution and water were added in a beaker and heated to about 60-70 ° C under stirring until complete dissolution of the surfactant. The final solution was allowed to cool to room temperature and the surfactant was added. The next step was to connect the pump to 24.95mL/min and to add the sodium silicate solution, water and surfactant in the previously protonated ion exchange column. The level of the column was maintained at a given level provided to ensure working at constant flow rate and the outlet of the column was collected in a beaker. The figure 7 shows the precipitate experiment 9:

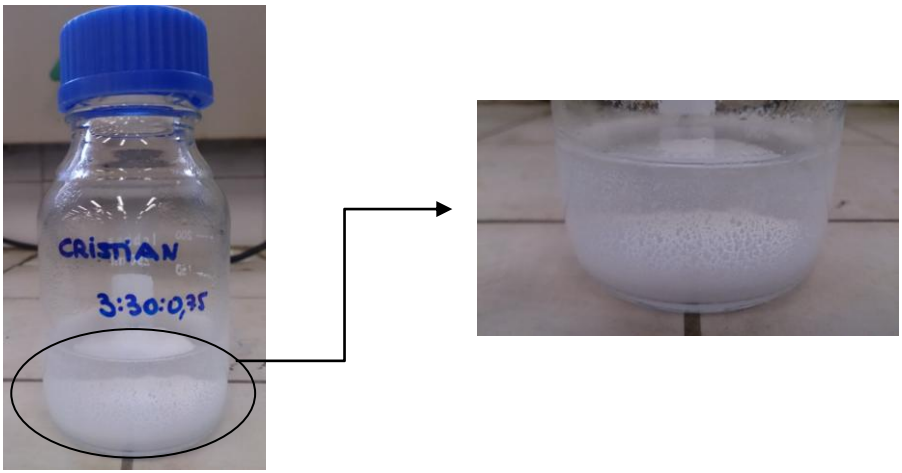

Figure 7. Precipitate of silica. Experiment 9 (3:30:0.75).

Once it reached the end time of operation, the column outlet was closed and the solution obtained from the column was introduced into a bottle to be left 24 hours in the oven at temperature of 105 ° C in order to achieve a white silica precipitate: the mesoporous material obtained.

Other hand, the column was washed with water and the resin was first regenerated with NaOH (1M) to dissolve the possible silica that may contain, after new water and finally regenerated with HCl (2M) which was the source of protons column. Once protonated, ion exchange column was prepared for a new experiment.

The next day, the bottle content's stove was filtrated using a vacuum pump and a Buchner funnel and the obtained silica material was left to dry at room temperature before being calcined. Finally, the material was calcined for 5 hours at 550 ° C to remove residual surfactant. The appearance of the material obtained was a white powder.

The following figure shows the appearance of some mesoporous materials obtained in the experiments shown by ion exchange column:

Figure 8. Appearance of mesoporous materials obtained in the ion exchange column. Experiment 1.

5.4. CHARACTERIZATION TECHNIQUES

5.4.1 Scanning Electron Microscope (SEM)

SEM (Scanning Electron Microscope) is a technique that provides a wide range of information from the sample surface. It is the most used method to study the surface topography and morphology of solids. It is also possible to observed agglomeration of the particles, the content of pores or open channels in the surface, etc.

Preparing the samples is an easy task which the main thing is to have a conductive solid sample. Otherwise, when the sample is not conductive, it is covered with a carbon film or thin metal fim such as gold to give conductive properties to the sample. In this case, work with mesoporous materials needs a specific sample preparation because the silica is not a conductive material (covered with carbon film). The process is done under vacuum to avoid the diversion of electrons through the air. The electrons can be dispersed through the sample or be projected with a determinate angle and energy and then collected on a brightness counter and its signal is used to generate an image on the screen.

Figure 9. Left: Material for preparation SEM. Right: sample holder with the mesoporous material.

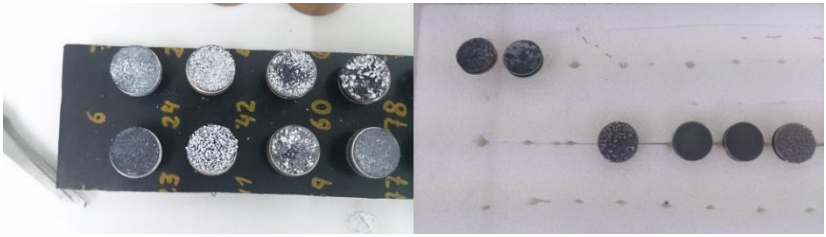

Figure 10. Left: sample holder with no carbon. Right: Sample holder with carbon.

The image provided by SEM is the result of an interaccion of a beam of electrons with a specific area of the sample surface (versus photons in the visible spectrum used in a microscopy). A tungsten filament is used as a light source because it makes a beam of electrons which falls on the sample.

Now, SEM microscope is shown:

Figure 11. SEM electron microscope. S-4100, HITACHI.

5.4.2. Transmission Electron Microscopy (TEM)

The transmission electron microscopy (TEM) is a technique used to obtain structural information from a nanoscale direct way. The fundamental difference between this microscopy and scanning aforementioned is that in the SEM images of the external morphology are obtained while the internal TEM morphology of solids is investigated and provides microstructural details.

The detectors of this microscopy are placed behind the sample in order to detect secondary electrons, the radio-scattered, X rays, transmitted electrons or elastically and inelastically combination of both, visible light photons, etc. Another notable difference is the maximum attainable resolution, higher for TEM ~ 0.1 nm, whereas for the SEM is ~ 1 nm.

The sample preparation should be done by depositing the material on a small ethanol suspension on a copper grid with a carbon film 300 mesh lattice. After drying the grid is introduced into the column JEOL JEM 2100 microscope operating at 200 kV with a detector of Si (Li) with an active area of 300 mm2 and a window ATW2.

Figure 12. Procedure Sample preparation for TEM.

The collection of images is done using a Gatan (model Orius) camera and analysis is done by computer software Digital Micrograph version 1.82.

Now, TEM microscope is shown:

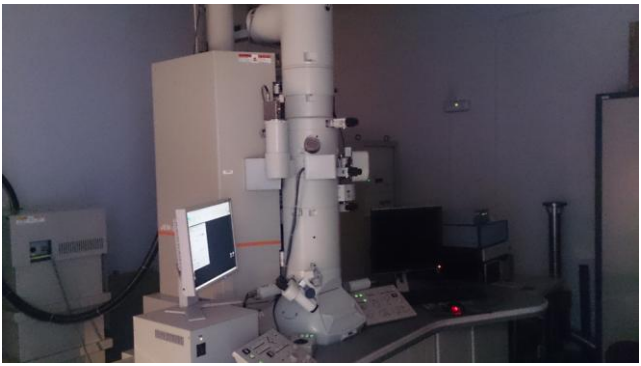

Figure 13. Transmission electron microscope (TEM). FEM-2100 Electron Microscope JEOL.

5.4.3. Multimolecular adsorption theory (BET)

The BET method or the theory multimolecular adsorption is a mathematical theory developed by Brunauer, Emmett and Teller in 1938. It is based on a kinetic model of the adsorption process proposed by Langmuir 1916 [37], wherein the solid surface is considered a distribution of equivalent adsorption sites. However, the Langmuir isotherm does not consider the possibility of layering of physisorption on initial (multilayer adsorption). This is the consequence to reach a saturation of the surface at high pressures. From Langmuir mechanism but introducing a number of amendments to simplify it, Brunauer, Emmett and Teller were able to develop currently known as BET equation, which admits the possibility of formation of multilayers, allowing the indefinite growth to occur condensing gas.

Regardless of their chemical composition, to characterize the pore structure of solids, the following parameters should be defined [39].

- Surface area (m^2/g): corresponds to the geometric extension of the surface of the walls of pores per gram of absorbant solid.
- Average pore diameter, dp (nm).
- Cumulative pore volume Vp (cm^3/g) total pore volume per gram of adsorbent.

The values of these parameters are obtained from the measurements of gas adsorption and desorption. The BET method can describe the physical adsorption of gas molecules on a solid surface. It is based on the adsorption of an inert gas (usually N_2 at low temperature) to determine the surface of a solid. BET method is one of the most used for the determination of surface areas and volumes of monolayer methods.

The results are displayed in adsorption-desorption isotherms, showing the amount of adsorbed gas (moles/g of adsorbent) as a function of the relative pressure P/Po (in the range of $0<P/P_o<P$. P corresponds to the equilibrium vapor pressure of the adsorbate and P_o the vapor pressure of the adsorbate pure liquid, at a specific temperature).

The IUPAC defines six types of adsorption isotherms. The BET theory is applicable to isotherms of type II (non-porous samples) or type IV (mesoporous). Otherwise, it is not possible to apply Type I isotherms (microporous samples), type III (non-porous samples with weak interaction with the gas), or type V (mesosporosas samples with weak interaction with the gas). Now, the field of application of the BET method generally is shown in isotherms II and IV (in shading).

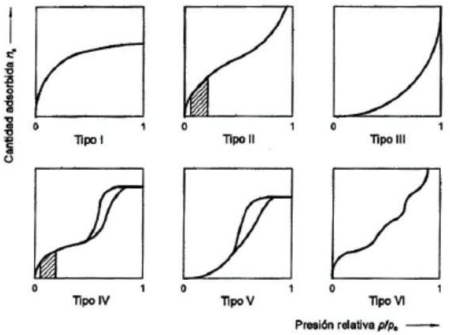

Figure 14. IUPAC classification of adsorption isotherm [40].

The sensitive range to be measured with the BET method is shaded II and IV Isotherm.

Among these six types of isotherms defined before, IV isotherm is important to study the characteristics of the mesoporous materials. It has a significant increase in adsorbed amount at intermediate pressure and goes through a filling mechanism in multilayers. Furthermore, the desorption process occurs differently from adsorption due to capillary condensation. Desorption

of gas absorbed same volume typically occurs at lower pressures, resulting in hysteresis. IUPAC, are classified into 4 types:

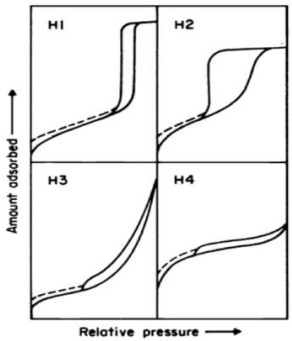

Figure 15. Classification exhibiting hysteresis adsorption-desorption isotherms of N_2 of IUPAC [41].

Figure 15 shows that according to the type of hysteresis:

- Type H1 shows the adsorption-desorption branches parallel and almost vertical. It comes in materials formed of agglomerates or compact spherical particles uniformly arranged. Usually, it indicates high uniformity of pore size and connectivity porous surface.

- The H2 type of triangular shape and a completely vertical desorption branch. This behavior was observed for inorganic oxides porous and attributed to the effects of connectivity porous, which are considered as a result of the presence of pores with narrow mouths (*ink-bottle pores*) or on materials with pores arranged as channels.

- H3 hysteresis in relative pressures close to the saturation pressure is not stabilized. It is associated with materials forming aggregates of flat particles ("platelike"), with pore-shaped plates.

- H4 type shows adsorption-desorption branches parallel and almost horizontal. This is associated with narrow slit-shaped pores, with the presence of microporosity.

The BET method involves determining the amount of gas adsorbed which is needed to cover the surfaces of accessible internal and external pores with a complete monolayer of adsorbate. Inaccessible pores are not detected [42].

The main idea of the BET method is to estimate the area of the solid once it is known the amount of adsorbed gas required to form a monolayer (the number of molecules forming the monolayer) and the area occupied by one of these adsorbed molecules.

To calculate the amount of adsorbed gas needed for forming a monolayer, n_a, the following equation is used:

$$\frac{P}{n(P^o - P)} = \frac{1}{n_a C} + \frac{C-1}{n_a C}\frac{P}{P_o} \qquad \text{(Equation 2)}$$

P/P_O : relative equilibrium pressure

n : the amount of gas adsorbed

C is a constant which is related to the heat of adsorption of the first monolayer. Defined as:

$$C = \frac{e^{(q_1 - q_L)}}{RT} \quad \text{(Equation3)}$$

q_1-q_L: net heat of adsorption

R: gas constant = 8.314 J / mol·K

T: absolute temperature in K

$P/n(P_0 - P)$ versus the relative pressure get $1/Cn_a$ as intercept and $(C-1)/Cn_a$ pending. Having these values, it is possible to calculate C and n_a.

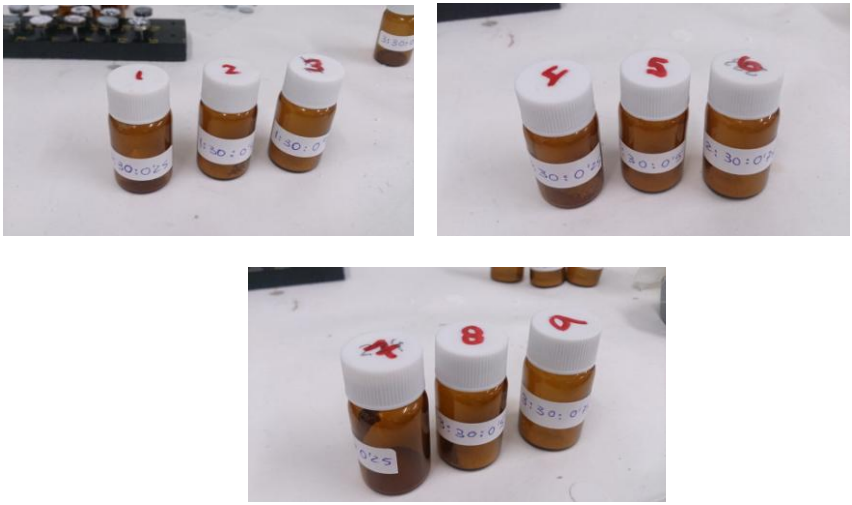

Figure 16. Samples to BET.

5.4.4. Small angle X-ray diffraction (SAXS)

The technique of X-ray diffraction is based on the incidence with a particular angle θ of a beam of X-rays on a flat sample. When X-rays impinge on the material, big part of this beam is scattered in all directions due to the electrons associated with atoms or ions in the path. However, the rest of the beam can bring x-ray diffraction, which occurs if there is an ordered arrangement of atoms and if the conditions (which are given by Bragg's law) are fulfilled (Eq. 4) [43] .

$$n\,\lambda = 2\,d_{hkl}\,sin\,\theta \quad \text{(Equation 4)}$$

It indicates the relationship between the spacing between two planes (d_{hkl}) wavelength (λ) and angle of diffracted X-ray beam (θ), n being an integer.

Generally, this technique is used in determining crystalline phases. In the mesostructured materials case, the regular arrangement of the pores produces reflections which appear as signals at low diffraction angles.

In Figure 17 the hexagonal structure of a mesoporous material (A) is represented P6mm symmetry and corresponding diffractogram (B) X-rays.

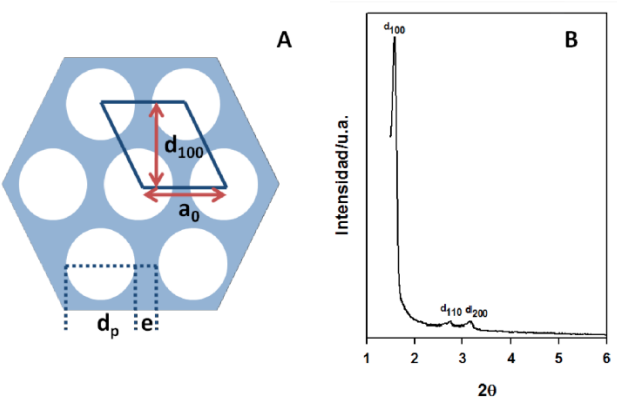

Figure 17. (A) hexagonal structure (B) X-ray diffractogram of a low angle mesoporous material with hexagonal symmetry P6mm [44].

Regarding the degree of structural order of these packed hexagonal materials, this technique allows evaluating by measuring the ratio of intensities of the diffraction signals d_{100} and d_{110}, being higher the order of the analyzed structure the larger is the ratio I_{110} / I_{100}.

These analyzes, also with Bragg's law, allows the calculation of the plane spacing in the crystallographic direction (100). It is calculated from the value of the unit cell a_0 through Eq. 5. As shown in Figure 17 (A), this value represents the distance between the centers of two adjacent pores in that direction which if they are combined with the DP parameter (pore diameter) obtained by the analysis of nitrogen adsorption, allows to determine the wall thickness (e) (Eq. 6).

$$a_0 = \frac{2\,d_{100}}{\sqrt{3}} \qquad \text{(Equation 5)}$$

$$e = a_0 - d_p \qquad \text{(Equation 6)}$$

The relationship between the peaks obtained by SAXS has been studied and it is known that as the type of structure which is obtained can be determinated according to the ratio of the peaks from the first peak, being valid for both the liquid crystal phases lyotropic as for structured mesoporous materials. Chart 4 summarizes these ratios:

Chart 4. Ratio spaced different phases of lyotropic liquid crystals [45].

Fase líquido cristalina	Relación de espaciados
Laminar	$1:\frac{1}{2}:\frac{1}{3}:\frac{1}{4}$
Hexagonal y hexagonal inversa	$1:\frac{1}{\sqrt{3}}:\frac{1}{\sqrt{4}}:\frac{1}{\sqrt{7}}:\frac{1}{\sqrt{9}}:\frac{1}{\sqrt{12}}:\frac{1}{\sqrt{13}}$
Cúbica micelar (grupo espacial Fm3m)	$1:\frac{1}{\sqrt{3}}:\frac{1}{\sqrt{4}}:\frac{1}{\sqrt{8}}:\frac{1}{\sqrt{11}}:\frac{1}{\sqrt{12}}:\frac{1}{\sqrt{16}}$
Cúbica micelar (grupo espacial Pm3n)	$1:\frac{1}{\sqrt{3}}:\frac{1}{\sqrt{4}}:\frac{1}{\sqrt{5}}:\frac{1}{\sqrt{8}}:\frac{1}{\sqrt{10}}:\frac{1}{\sqrt{12}}:\frac{1}{\sqrt{13}}:\frac{1}{\sqrt{14}}:\frac{1}{\sqrt{16}}$
Cúbica micelar inversa (grupo espacial Fd3m)	$1:\frac{1}{\sqrt{3}}:\frac{1}{\sqrt{8}}:\frac{1}{\sqrt{11}}:\frac{1}{\sqrt{12}}:\frac{1}{\sqrt{16}}$
Cúbica bicontinua inversa (grupo espacial Im3m)	$1:\frac{1}{\sqrt{2}}:\frac{1}{\sqrt{4}}:\frac{1}{\sqrt{6}}:\frac{1}{\sqrt{8}}:\frac{1}{\sqrt{10}}:\frac{1}{\sqrt{12}}:\frac{1}{\sqrt{14}}:\frac{1}{\sqrt{16}}$
Cúbica bicontinua inversa (grupo espacial Pn3m)	$1:\frac{1}{\sqrt{2}}:\frac{1}{\sqrt{3}}:\frac{1}{\sqrt{4}}:\frac{1}{\sqrt{6}}:\frac{1}{\sqrt{8}}:\frac{1}{\sqrt{9}}:\frac{1}{\sqrt{10}}:\frac{1}{\sqrt{12}}:\frac{1}{\sqrt{14}}$
Cúbica bicontinua inversa (grupo espacial Ia3d)	$1:\frac{1}{\sqrt{6}}:\frac{1}{\sqrt{8}}:\frac{1}{\sqrt{14}}:\frac{1}{\sqrt{16}}$

Because of fine powder structure of mesoporous materials, they were prepared in capillaries (used 1mm diameter with wall thickness of 0.01mm).

6. RESULTS

This project has studied the influence of relations surfactant, sodium silicate and water in the synthesis of a mesoporous material by ion exchange column. The main objective was to obtain a mesoporous material with the highest possible degree of order to maximize their surface area. The Ion exchange column is used to study the industrial feasibility of the process of obtaining the ordered mesostructured silica currently carried out with an acidic medium presenting some potential disadvantages that are avoided by using exchange column ion.

As already mentioned, mesoporous materials ordinands are characterized by a high specific surface areas and provide the ability to modify their properties by making small changes in the parameters of synthesis. This lead to the physicochemical characteristics of such materials may be chosen by other synthesis parameters and not explicitly with the choice of surfactant which provides the template for the mesopores.

Since nowadays, it has been common to use TEOS and TMOS in the synthesis of these materials. There are two reactions: hydrolysis and condensation, which are competitive, and with the release of alcohol contributes to the difficulty of formation material. The medium in which the synthesis of the material is done is important due to the fact that the pH changes the rate of condensation of the silica and alters the particle morphology because of the action of the acid counterion which can change the shape of the surfactant micelles [46].

It is also rellevant to highlight the importance of the nature of the nonionic surfactant. Pluronic P84 was chosen in this project which it belongs to the family of triblock ethylene and removes from the material and cheaper than ionics. These are the advantages from the industrial viewpoint.propylene oxides. Nonionic surfactants are biodegradable, have no toxicity and are easier to remove from the material and cheaper than ionics. These are the advantages from the industrial viewpoint.

6.1. RUPTURE CURVES OF THE ION EXCHANGE COLUMN

The knowledge of the rupture curves is essential to design the ion exchange column. Generally, the rupture curves must be determined experimentally, due to the difficulty of prediction. In this project, they represent the evolution of the pH of the solution leaving the column in front of time. The curves represent 5 to 95% use of the column which it mens to obtain a pH value of about 95% of the initial pH value. Charts 8, 9, 10 on the Appendix show the relationship between time and pH mL solution of sodium silicate and water obtained working at constant flow of 24.95 mL/min.

Rupture time is called the time elapsed since the beginning of the operation in the column until the solution ions appear in the output current or more specifically when the allowable necessary pH is reached in each solution. Before the rupture time, the ion exchange happens in the column and in that moment there are no ion exchange columns. Therefore, the output and the input of the column contain the sodium silicate solution.

Nine experiments with three different ratios of silicate solution to water (1:30, 2:30 and 3:30) were performed. The experimental procedure for obtaining the rupture curves has been explained. The results are presented below:

Chart 5. Initial data for rupture curves.

Mass ratio [g]		**Mass [g]**			
Sodium silicate	Water	Sodium silicate	Water	**Replica**	**pH initial**
1	30	22.58	677,42	1	10.82
				2	10.88
2	30	43.75	656,25	1	11.23
				2	11.27
3	30	63.64	636,36	1	11.80
				2	11.95

Finally, the three rupture curves with its two replicas are shown below:

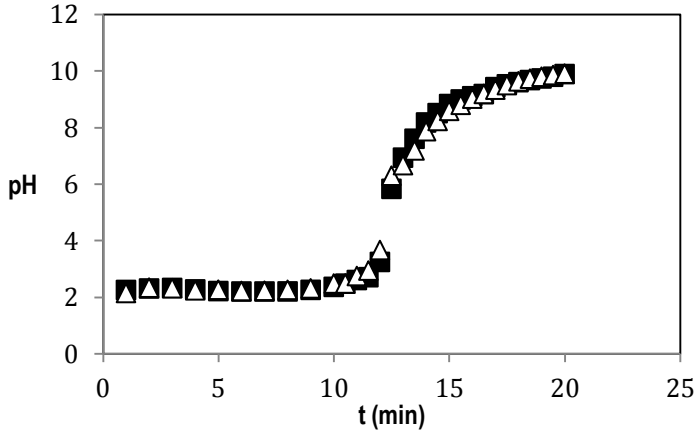

Figure 18. Rupture curve for sodium silicate and water ratio of 1:30 at 24.95 mL/min. Replica 1 (black squares), replica 2 (white triangles).

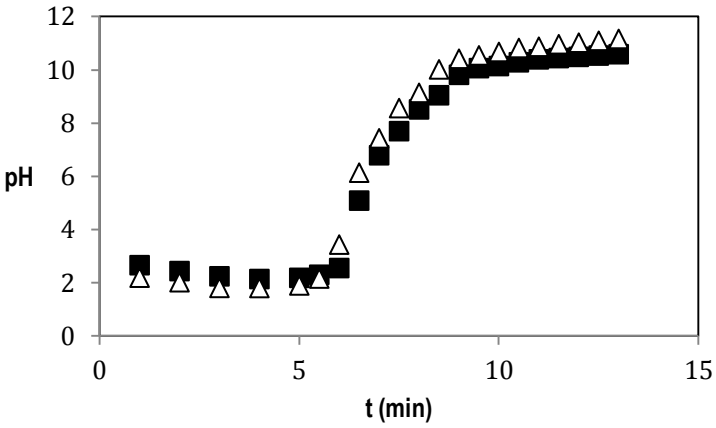

Figure 19. Rupture curve for sodium silicate and water ratio of 2:30 at 24.95 mL/min. Replica 1 (black squares), replica 2 (white triangles).

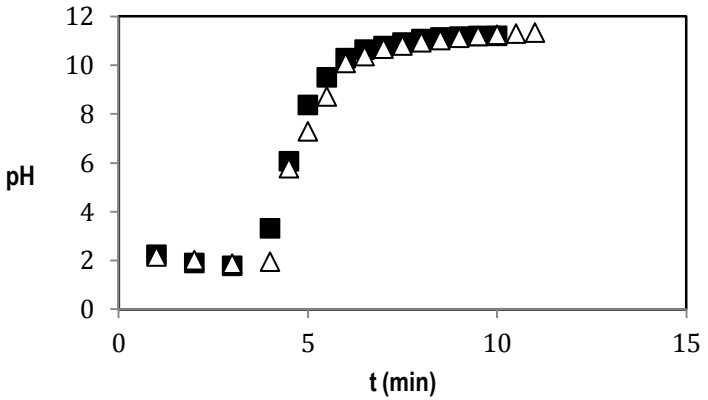

Figure 20. Rupture curve for sodium silicate and water ratio of 3:30 at 24.95 mL/min. Replica 1 (black squares), replica 2 (white triangles).

In figures shown before, it is possible to see that the two replicas performed for each of them are almost equal as the results are similar and there are no significant differences. Comparison of the three rupture curves of the three different ratios of silicate:water are shown below (figure 21):

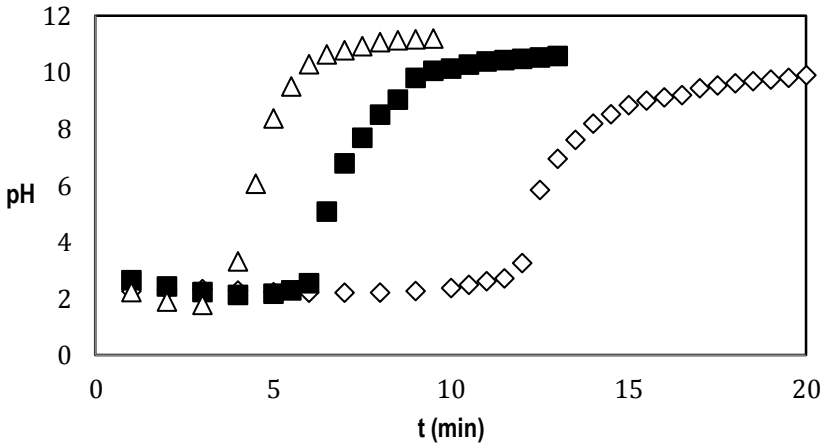

Figure 21. Rupture curves of three sodium silicate:water ratios. Ratio of 1:30 (white rhombus), ratio of 2:30 (black squares), ratio of 3:30 (white triangles).

In figure 21 it is possible to see that the rupture time is less for the ratio 3:30, followed by 2:30 and finally the ratio 1:30 silicate:water ratio. The results are as expected because working with constant flow for the three ratios expects that the ratio 3:30 has a shorter rupture time as it contains a higher ratio of sodium silicate and therefore time ion exchange is lower. For the same reason, the ratio 2:30 is the second lower rupture time and thus the ratio 1:30 gets a longer break.

According to the progress of the solution through the resin, changes were observed in the hue of the resin. The protonated resin (prior HCl solution) adopted a brown-orange color, similar to honey color. Such phenomenon can be explained so that the column layout was thought to work in plug flow, allowing seeing color variations in each volume differential to the length of the column. Therefore, when sodium silicate solution was flowing through the ion exchange column, the resin was acquiring a darker brown shaped plug flow. When the ion exchange column was treated with NaOH to dissolve such residual silica, it was possible to see another important change in appearance: a dark reddish-brown at the end because the resin containing no protons.

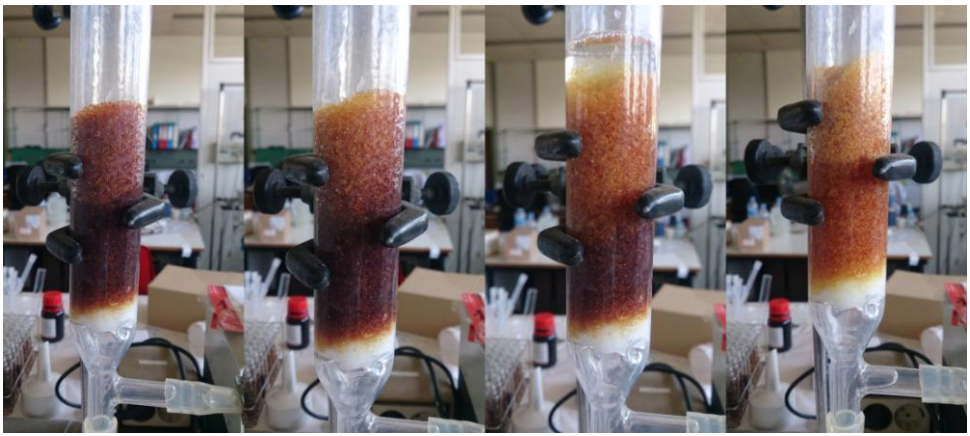

Figure 22. Evolution from desprotonaed resin to protonated resin.

These results validate the three rupture curves. It is possible to extract the information necessary from these data to restrict the time conditions in the later varieties of mesoporous silica material through the ion exchange column.

6.2. MESOPOROUS MATERIALS SYNTHESIZED BY ION EXCHANGE RESIN COLUMN

To obtain ordered mesoporous materials in the ion exchange column, there were chosen three different sodium silicate rations of 1, 2 and 3; three different surfactant ratios 0.25, 0.50 and 0.75 and finally the same ratio of water of 30 for 3 experiments. The reason of this choice was following the final degree of Jennifer Alegre Miranda: "*Study of the preparation of mesoporous silica materials by ion exchange resin*". In order to have a safety margin and ensuring the correct obtaining mesoporous material, the pH should be less than 2 (acid pH). Experiments are shown in the table below in more detail, and the operation time of each one and their corresponding pH obtained at the end.

Chart 6. Experiments performed in ion exchange column and their properties.

				Mass ratio [g]			**Mass [g]**		
Experiment	**t operation [min]**	**Final volum [mL]**	**Final pH**	Sodium silicate	Water	Surfactant	Sodium silicate	Water	Surfactant
1	8.5	212.08	1.634	1	30	0.25	9.60	288.00	2.40
2	8.5	212.08	1.599	1	30	0.5	9.52	285.72	4.76
3	8.5	212.08	1.640	1	30	0.75	9.45	283.46	7.09
4	4.5	112.28	1.545	2	30	0.25	12.40	186.05	1.55
5	4.5	112.28	1.678	2	30	0.5	12.31	184.60	3.08
6	4.5	112.28	1.548	2	30	0.75	12.21	183.21	4.58
7	3	74.85	1.721	3	30	0.25	11.28	112.78	0.9
8	3	74.85	1.699	3	30	0.5	11.19	111.94	1.87
9	3	74.85	1.682	3	30	0.75	11.11	111.11	2.78

6.2.1 BET Results

Accordding to IUPAC [41] N_2-adsorption-desorption isotherms of the obtained materials correspond to type IV isotherms. This kind of isotherms are typically of the mesoporous materials, characterized by a shoulder form at low relative pressures and a hysteresis loop that starts at p/p_0 values of 0.42 approximately. Figures 35-43 on Appendices 2 shown the N_2-adsorption-desorption isotherms of experiments. The loop type is H2 which indicate the presence of pores at mesoscale range. BET surface specific area is obtained from the isotherm data.

The following table summarizes shows the BET data obtained:

Chart 7. Results of the materials synthesized in the ion exchange column and properties.

	Mass ratio [g]				
Experiment	Sodium silicate	Water	Surfactant	**Diameter [Å]**	**Specific surface [m^2/g]**
1	1	30	0.25	40	450
2	1	30	0.50	40	398
3	1	30	0.75	40	419
4	2	30	0.25	40	481
5	2	30	0.50	40	575
6	2	30	0.75	40	508
7	3	30	0.25	40	345
8	3	30	0.50	40	232
9	3	30	0.75	40	355

The comparison of the influence of surfactant P84 and the influence of sodium silicate over the surface area finally obtained in silica mesoporous materials obtained in the synthesis of these materials by ion exchange column were shown in figures 23 and 24:

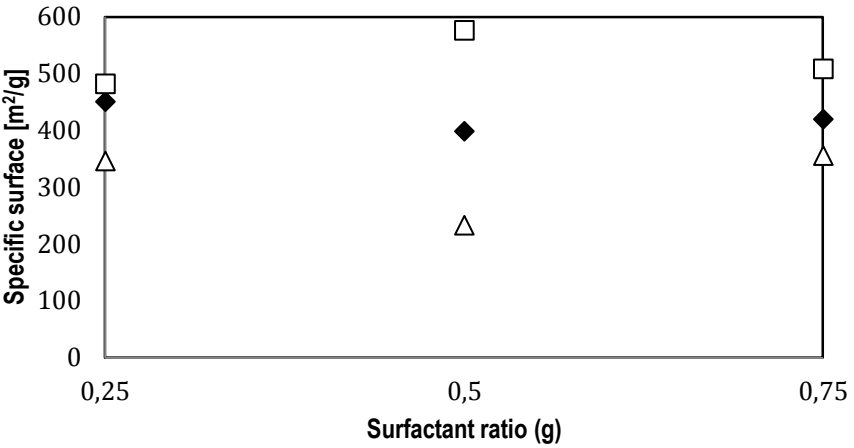

Figure 23. Specific surfaces in front of surfactant:water ratio. Ratio of 1:30 (black rhombus), ratio of 2:30 (white squares), ratio of 3:30 (white triangles).

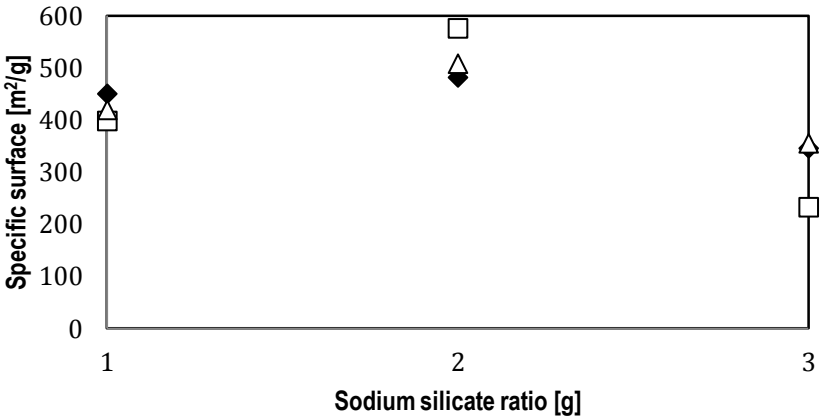

Figure 24. Specific surfaces in front of water:sodium silicate ratio. Ratio of 30:0.25 (black rhombus), ratio of 30:0.50 (white squares), ratio of 30:0.75 (white triangles).

Analyzing the figures it seems that the amount of sodium silicate significantly influence in the surface area of the mesoporous materials obtained. Regarding the amount of surfactant, no influence can be seen in the studied range

Figure 23 shows the influence of the amount of sodium silicate solution used in each experiment with the specific surface of the material obtained. It is noted that the larger specific surface is obtained in relation with the intermediate silicate:water ratio (the ratio 2:30). After this, the best value is the smallest ratio 1:30. The trend can be explained because the sodium silicate condenses around the micelles of surfactant as rods or cylinders, the excess or deficiency silicate causes that not all the silica can condense neatly around the micelles, and thus, condense amorphous silica and covering uncontrolled surfactant structures causing an ordination decrease.

A statistical analysis is done with the "Statgraphics 4.1 Plus" program in order to determine which variables studied in experimental design significantly influence the specific area and pore diameter. The following figure shows the resulting Pareto chart for the specific area.

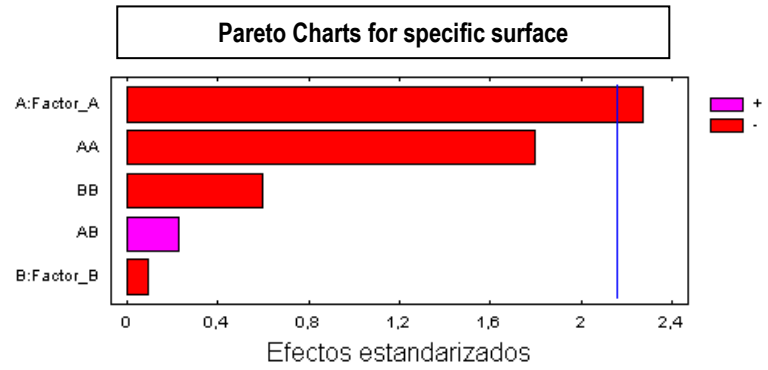

Figure 25. Pareto charts**.** Where the factor A is the ratio of sodium silicate, the ratio factor B is the relation of surfactant.

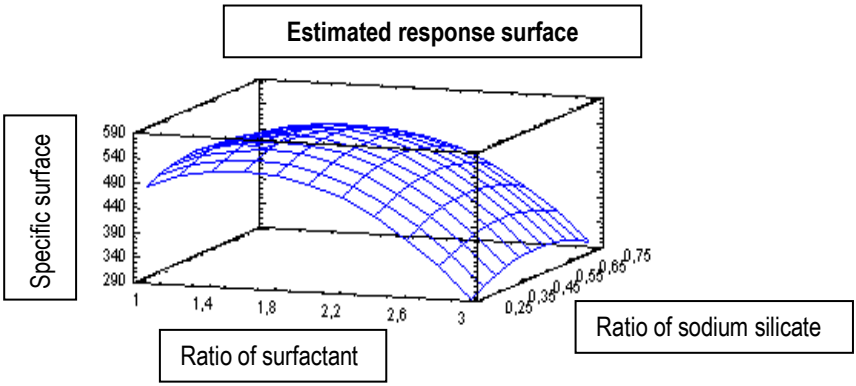

Figure 26. Estimated response surface of material's specific surface area in front of surfactant and sodium silicate ratios.

Analyzing the Pareto chart and the estimated response surface, it is possible to determinate that for the synthesis of mesostructured silica in the ion exchange column there is a variable that significantly influences on the material's bet surface in the studied range. This variable is the factor A which is the ratio of sodium silicate used in the synthesis of mesoporous material.

In the response surface it is possible to see that a maximum is obtained in the specific surface. It is expected that in the range studied, silicate:water:surfactant ratios are obtained and the specific surface is maximized.

6.2.2. TEM Results

The following images compare the results of the nine experiments 9 with the 9 images taken in 40.000 increases provided to compare between them:

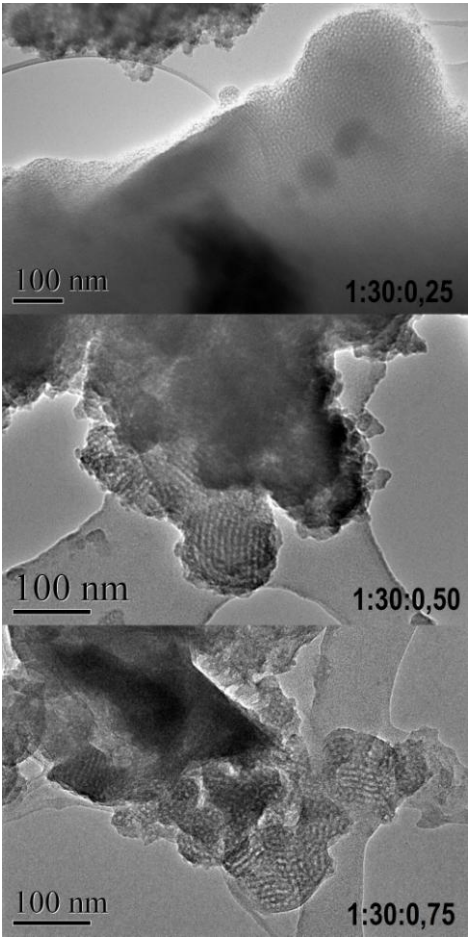

Figure 27. TEM figures from ratio of 1:30.

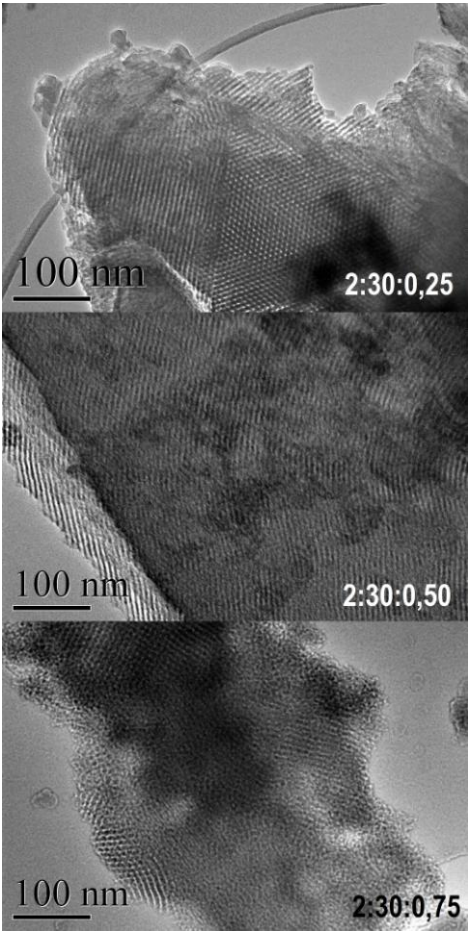

Figure 28. TEM figures from ratio of 2:30.

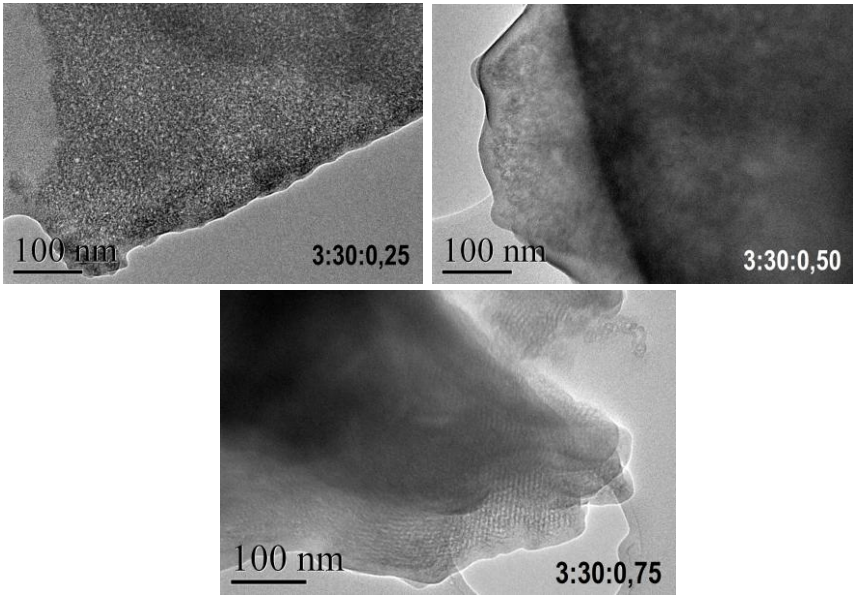

Figure 29. TEM figures from ratio of 3:30.

With the comparison of images of TEM, it is possible to say that the most ordered mesoporous materials that have been obtained are central experiments regarding sodium silicate: water 2:30. As it goes to the ends of the experiments it can be seen that there are areas of lower order. TEM images confirm again the results of BET because the core material is the highest order and hence higher surface area.

In the following images, ordinations obtained samples are shown. In the figures 30, 21 and 32 the management of materials experiments 2, 4 and 5 at different scales are summarized:

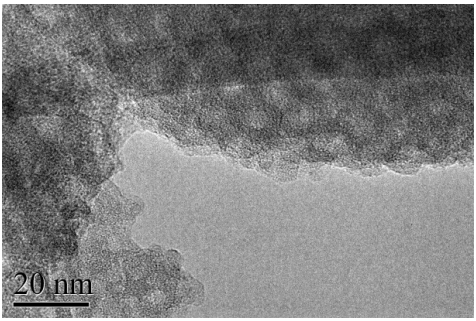

Figure 30. Ordination of experiment 2 (1:30:0.50.)

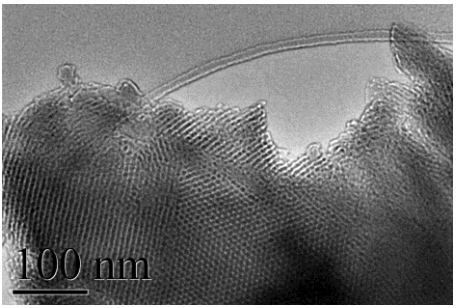

Figure 31. Ordination of experiment 4 (2:30:0.25).

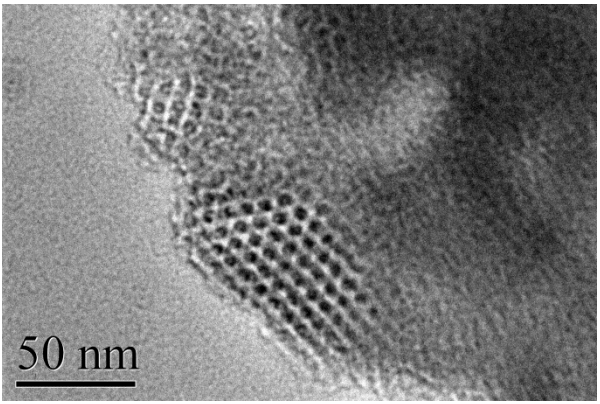

Figure 32. Ordination of experiment 5 (2:30:0.50).

As it can be seen in the three previous images, ordination obtained is a honeycomb type, typical of the hexagonal arrangement.

6.2.3. SEM results

Subsequently, figures SEM images for six of the nine materials synthesized by ion exchange column are shown.

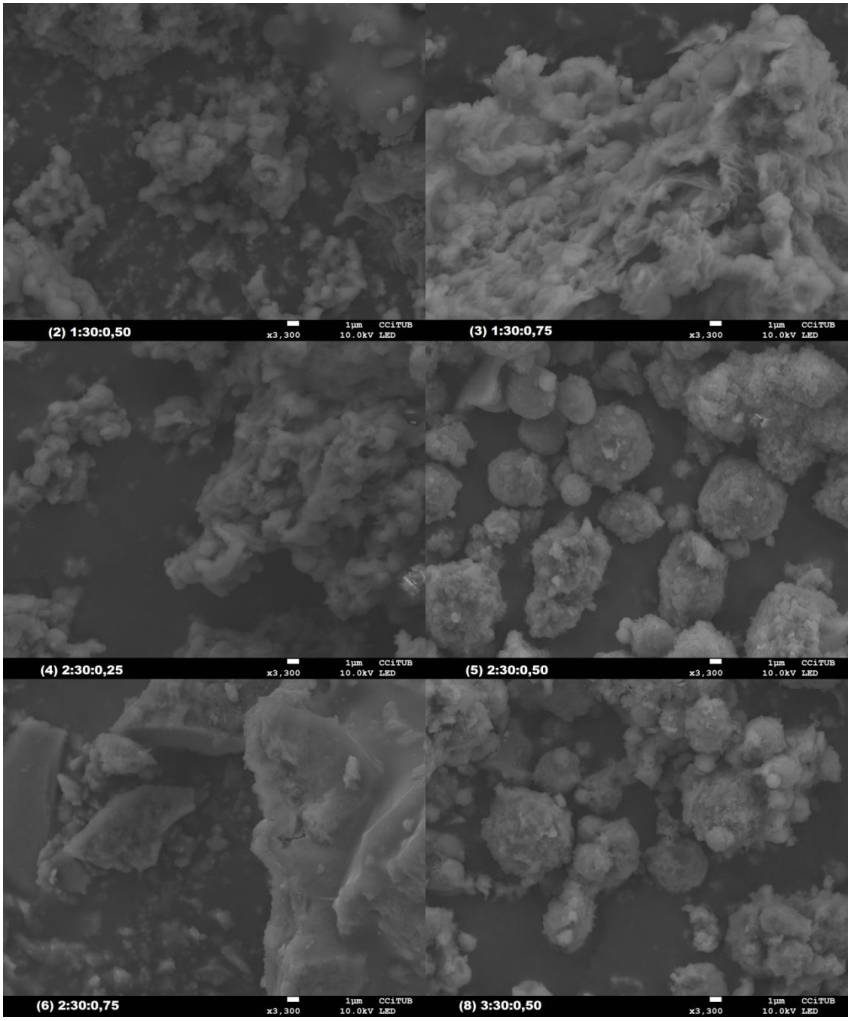

Figure 33. Comparison of different SEM results.

In the figure, it can be seen that the morphology of materials is similar: silica morphology similar to that of small spheres which are agglomerated and independent of management pores.

6.2.4. SAXS Results

In order to discern, the pore structure of the experiments the samples 4, 5, 6 and 8 to SAXS and diffractograms obtained are shown below:

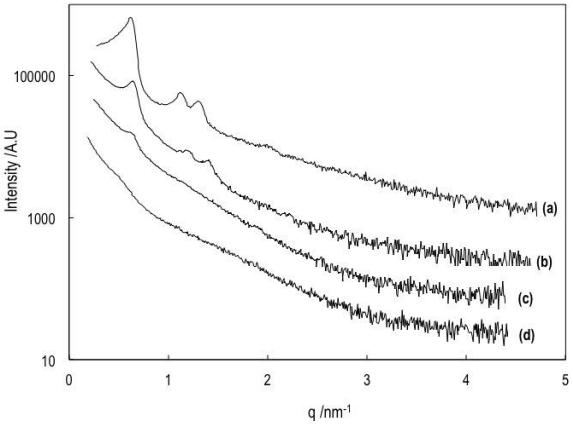

Figure 34. SAXS diffractograms for experiments.

Experiment 5: 2:30:0.50. (a)

Experiment 4: 2:30:0.25. (b)

Experiment 6: 2:30:0.75. (c)

Experiment 8: 3:30:0.50. (d)

It is possible to see three different peaks in the results of experiment at (2: 30: 0.50). The first peak is at q_1=0.65nm^{-1}, the second peak q_2=1.10nm^{-1} and the third peak in q_3=1.30nm^{-1}. These results provide a list of equally spaced from:

$$\frac{q_1}{q_1}:\frac{q_1}{q_2}:\frac{q_1}{q_3} = \frac{0{,}65}{0{,}65}:\frac{0{,}65}{1{,}10}:\frac{0{,}65}{1{,}30} \approx 1:\frac{1}{\sqrt{3}}:\frac{1}{\sqrt{4}}$$

In the first two cases (a and b results), the three clear peaks have a spaced ratio of 1: 1/√ 3: 1/√4 corresponding to a hexagonal structure among others. The other structures that provide this peak ratio are micelle cubic Fm3m or Pm3n. TEM images of figures 30, 31, 32 showed an undoubtedly hexagonal arrangement due to the structure of bee panel type which is typical of

hexagonal structures. Therefore, it is possible to conclude that the ordered structural of P84 is likely to be hexagonal

By contrast in the results of experiments 6 ((c) plot in figure 34) only showed one peak. This could be explained because not all the material is ordered as can be seen in TEM images. In this material ordered zones and disordered zones coexist. Experiment 6 has the same silicate ratio but highest surfactant ratio so it could be that an excess of surfactant provokes that it could not arrange properly (there are a lot of micelles that disturb each other and they cannot be arranged in form of cylinders or rods) and the structure is not formed correctly.

7. CONCLUSIONS

The aim of this project, entitled "*Use of ion exchange column to Obtain ordered mesoporous materials*", was to obtain ordered mesoporous materials silica from sodium silicate and use a ion exchange column in the synthesis process to incorporate the synthesis of silica materials in an industrial level.

The study focused on examining the influence of surfactant:water ratio and sodium silicate:water on the value of the specific surface area obtained of mesoporous materials previously while characterizing materials synthesized by characterization techniques.

The conclusions drawn from the study are:

1) Ion exchange columns are possible alternatives in the process of synthesis of silica ordered mesoporous materials because within the range of work and study, it has been possible to obtained mesoporous materials with pores arranged in the space, maximizing the value of the specific surface of the material.

2) It has been concluded that the surfactant:water ratio does not appear to be a significant factor in the synthesis of silica materials within the range studied.

3) By contrast, it has been concluded that the ratio of sodium silicate:water shows a significant factor within the range studied. It has been found that a maximum specific surface area for a ratio of sodium silicate:water is obtained. It may be due to the excess or defect of sodium silicate in synthetic processes. A defect of sodium silicate can cause that there is no enough silicate to cooperate with all the surfactant in order to form the ordered mesostructure. Conversely, an excess of sodium silicate may cause an amorphous silica precipitate causing disordered structure.

4) Ion exchange columns seem to be a good alternative to take the process of synthesis of mesoporous silica materials on an industrial scale because they have the possibility of obtaining silica materials with pores arranged in space. It is also possible to avoid the washing step in the synthesis of mesostructured silica materials.

8. REFERENCES AND NOTES

1. Sing, K. S. W.; Everett, D. H.; W. Haul, R. A.; Moscou, L.; Pierotti, J.; Rouquerol, J.; Siemieniewska, T. Pure *Appl. Chem*. **1985**, 57, 603.

2. C.T. Kresge, M.E. Leonowicz, W.J. Roth, J.C. Vartuli, J.S. Beck. "*Nature*" 359, **1992**, 710.

3. Y. Tao, H. Kanoh, L. Abrams, K. Kaneko, *Chem. Rev.* 106, **2006**, 896.

4. F. Di Renzo, H. Cambon, R. Dutartre, Micropor. Mater. 10, **1997**, 283.

5. T. Yanagisawa, T. Shimizu, K. Kuroda, C. Kato, C. Bull. "*The Preparation of Alkytrimethylammonium-Kanemite Complexes and Their Conversion to Microporous materials*". Chem. Soc. Jpn. **1990**, 63, p.988.

6. Silaghi, M.-C., Chizallet, C., Raybaud, P.; "*Challenges on molecular aspects of dealumination and desilication of zeolites, Microporous and Mesoporous Materials*", 191. **2014**, 82-96.

7. Mesoporous materials: tunable structure, morphology and composition.

8. Gregori M., Patricia Benito P., Giusseppe F., Migani M., Millefanti S., Ospitali, F, Albonetti S, "*Preparation of Pd/Cu MCM-41 catalysts*", **2014**, 1-9, 190.

9. J. S. Beck, J. C. Vartuli, W. J. Roth, M. E. Leonowicz, C. T. Kresge, K. D. Schmitt, C. T. W. Chu, D. H. Olson, E. W. Sheppard, S.B. McCullen, J.B. Higgins, J.L.. Schlenker, J. Am. *Chem. Soc*, **1992**, 114, 10834 – 10843.

10. Iler, R. K. "*The chemistry of silica: solubility, polymerization, colloid and surface properties, and biochemistry*"; Wiley, **1979**.

11. Mihranyan, A.; Ferraz, N.; Strømme, M. Progress in Materials Science. **2012**, 57, 875-910.

12. Schubert, U.; Hüsing, N. "*Synthesis of inorganic materials*"; Wiley-VCH, **2005**.

13. Arvanitidou, E.; Boyd, T.J.; Fruge, L.; Gaffar, A. Viscio, D.; Xu, G. US 20070020201.

14. Banowski, B.; Foerster, T.; Heller, M. Kropf C. DE 10028207.][Giroud, F.; Nocerino, C.; Sturlag, J. FR 2814068

15. Tsai, M. WO 2010091529

16. Chen, J.; Mcginnis, J.F.; Patil, S.; Seal, S.; Sezate, S.; Wong, L. US 20070202193.

17. Jain, S.K.; Jain, N.K. Multiparticulate carriers for sun-screening agents, Int. J.Cosmet. Sci. **2010**, 32, 89–98

18. Wissing, S.A.; Müller, R.H. "*Solid lipid nanoparticles as carrier for sunscreens: in vitro release and in vivo skin penetration*", J. Controlled Release. **2002**, 81, 225–233.

19. Frerichs, S.R.; Morrison, W.H. US 20050129634.

20. Sun, W.; He, Q.; Luo, Y. Mater Lett. **2007**, 61, 1881

21. Schlumpf, M.; Cotton, B.; Conscience, M.; Haller, V.; Steinmann, B.; Lichtensteiger, W. Environ. Health Persp. **2001**, 109, 239.

22. Chen-Yang, Y.W.; Chen, Y.T.; Li, C.C.; Yu, H.C.; Chuang, Y.C.; Su, J.H.; Lin, Y.T. "*Preparation of UV-fillter encapsulated mesoporous silica with high sunscreen ability*". Materials Letters. **2011**, 65, 1060-1062.

23. Jaroenworalucka, A.; Pijarna, N.; Kosachana, N.; Stevens, R. "*Nanocomposite TiO2–SiO2 gel for UV absorption*". Chemical Engineering Journal. **2012**, 181-182, 45-55

24. Leal-Calderon, F.; Schmitt, V.; Bibette, J. Emulsion Science: Basic Principles , 2nd ed.; Springer: New York, **2007**.

25. Osterholtz, F.D.; Pohl, E.R. "*Kinetics of the hydrolysis and condensation of organofunctional alkoxysilanes: a review*". J. Adhesion Sci. Technol., **1992**, 6, 127-149.

26. Ferguson, J.; Kemblowski, Z. Applied Fluid Rheology, 1st ed.; Elsevier applied science: Barking, **1991**.

27. Argyo C., Weiss V., Bräuchle C., Bein T., "*Multifunctional Mesoporous Silica Nanoparticles as a Universal Platform for Drug Delivery*", **2014**, 26 (1), 435-451.

28. Wan, Y.; Zhao, D. Y. Chem. Rev. **2007**, 107, 2821.

29. Wright, P. A., "*Microporous Framework Solids*", RSC Publishing, **2008**.

30. Yaghi, O. M.; Li, G. M.; Li, H. L. "*Nature*" **1995**, 378, 703.

31. Beck, J. S.; Vartuli, J. C.; M.E, L.; C.T, K.; Schmitt, K. D; Chu, C. T. W.; Olson, D. H.; Sheppard, E. W.; McCullen, S. B.; Higgins, J. B.; J.L, S. J. Am. Chem. Soc **1992**, 114, 10834.

32. Doadrio, J. C.; Sousa, E. M. B.; Izquierdo-Barba, I.; Doadrio, A. L.; Perez-Pariente, J.; Vallet-Regi, M. J. Mater. Chem. **2006**, 16, 462.

33. Vallet-Regi, M.; Balas, F.; Arcos, D. Angew. Chem. Int. Ed. **2007**, 46, 7548.

34. Beck, J.S., et al. J. Am. Chem. Soc., **1992**. 114, p. 10834-10843

35. Hines, A.L. y Maddox, R.M. "Mass Transfer. Fundamentals and Applications", **1985**.

36. McCabe, W.L.; Smith, J.C. y Harriot, P. "*Operaciones unitarias de Ingeniería Química*", **1994**.

37. Perry, R.H. y Green, D.W. "*Manual del ingeniero químico*", **2011**, Vol. III.

38. C. Boissière, A. Larbot, A. Van der Lee, P.J. Kooyman, É. Prouzet, Chem. Mater. 12, **2000**, 2902.

39. E. Santamaría, A. Maestro, M. Porras, J.M. Gutiérrez, C. González. Chemical Engineering Journal 226, **2013**, 7-12.

40. K. Unger, Angew. Chem. Int. Ed., 11, **1972**, p 267-278.

41. S. Brunauer, P. H. Emmett y E. Teller, , J.Chem. Soc. Chem., 60, **1938**, p 309- 319

42. P.A. Monson. Microporous and Mesoporous Materials, 160, **2012**, 47-66.

43. V. Pávlov in Física del Estado Sólido, ed. Bibfismat, 1st edn., **1985**.

44. V. Meynen. "*Microporous and Mesoporous Materials*", 125, **2009**, 170–223.

45. A. Paschalis, U. Olsson, B. Lindman; Langmuir, **1998**, 14, 2627-2638.

46. P. Atkins y J. Padua, Physical Chemistry, Oxford University Press, 7th edn., **2002**.

9. ACRONYMS

P84 - Pluronic P84

TEOS - Tetraethyl orthosilicate → $Si(OC_2H_5)_4$

TMOS - Tetramethyl orthosilicate → $Si(OCH_3)_4$

CMC - Critical micelle concentration

LCT - Liquid crystal template

CSA - Cooperative Self-Assembly

TEM - Transmission Electron Microscopy

SEM - Scanning Electron Microscope

BET - Brunauer-Emmet-Teller

SAXS - Slow angle X-ray diffraction

HCl - Hydrochloric acid

NaOH - Sodium hydroxide

MCM - Mobil Composition of Matter

IUPAC - International Union of Pure and Applied Chemistry

APPENDICES

APPENDIX 1: RUPTURE CURVES

Chart 8. pH evolution in front of time for ratio 3:30.

Replica 1		Replica 2	
t (min)	pH	t (min)	pH
1	2.23	1	2.16
2	1.894	2	2.009
3	1.777	3	1.865
4	3.313	4	1.947
4.5	6.059	4.5	5.776
5	8.366	5	7.285
5.5	9.497	5.5	8.715
6	10.283	6	10.087
6.5	10.631	6.5	10.368
7	10.777	7	10.672
7.5	10.921	7.5	10.8
8	11.064	8	10.935
8.5	11.13	8.5	11.024
9	11.164	9	11.117
9.5	11.192	9.5	11.193
10	11.197	10	11.242

Chart 9. pH evolution in front of time for ratio 2:30.

Replica 1		Replica 2	
t (min)	pH	t (min)	pH
1	2.648	1	2.18
2	2.427	2	2.01
3	2.23	3	1.797
4	2.128	4	1.793
5	2.172	5	1.889
5.5	2.289	5.5	2.148
6	2.541	6	3.423
6.5	5.074	6.5	6.124
7	6.778	7	7.414
7.5	7.683	7.5	8.549
8	8.5	8	9.123
8.5	9.031	8.5	10.003
9	9.799	9	10.403
9.5	10.05	9.5	10.529
10	10.128	10	10.658
10.5	10.27	10.5	10.808
11	10.38	11	10.854
11.5	10.428	11.5	10.948
12	10.473	12	11.006
12.5	10.522	12.5	11.077
13	10.573	13	11.147

Chart 10. pH evolution in front of time for ratio 1:30.

Replica 1		**Replica 2**	
t (min)	pH	t (min)	pH
1	2.262	1	2.156
2	2.313	2	2.345
3	2.333	3	2.325
4	2.281	4	2.25
5	2.223	5	2.271
6	2.207	6	2.228
7	2.207	7	2.235
8	2.21	8	2.267
9	2.265	9	2.319
10	2.371	10	2.491
10.5	2.485	10.5	2.492
11	2.613	11	2.756
11.5	2.713	11.5	2.949
12	3.253	12	3.674
12.5	5.837	12.5	6.303
13	6.939	13	6.676
13.5	7.608	13.5	7.197
14	8.183	14	7.877
14.5	8.514	14.5	8.239
15	8.835	15	8.595
15.5	8.997	15.5	8.809
16	9.11	16	9.027
16.5	9.19	16.5	9.194
17	9.433	17	9.345
17.5	9.533	17.5	9.506
18	9.609	18	9.639
18.5	9.683	18.5	9.733
19	9.74	19	9.802
19.5	9.801	19.5	9.861
20	9.895	20	9.911

APPENDIX 2: ADSORPTION ISOTHERMS

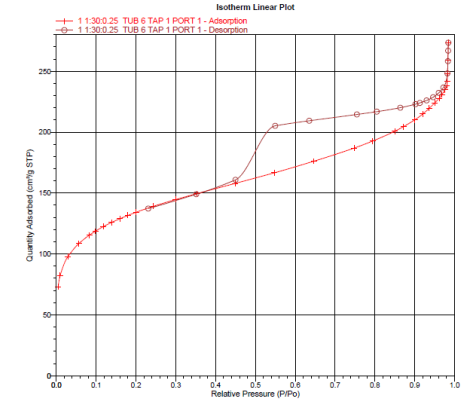

Figure 35. Isotherm of Experiment 1 (1:30:0.25)

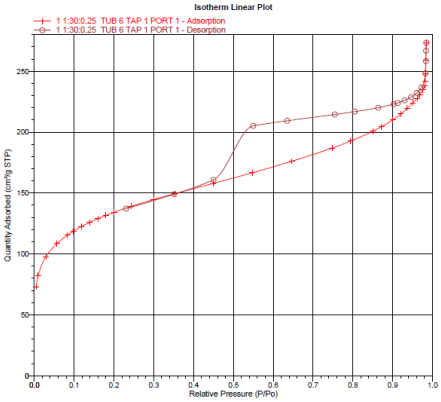

Figure 36. Isotherm of Experiment 2 (1:30:0.50)

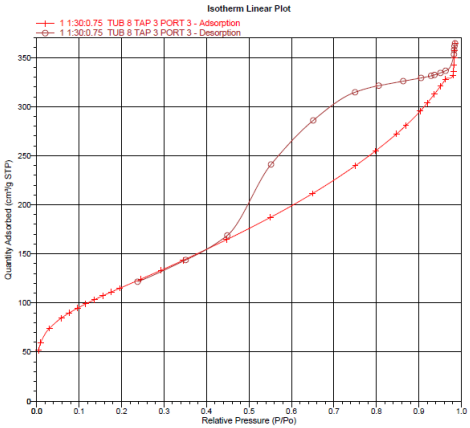

Figure 37. Isotherm of Experiment 3 (1:30:0.75)

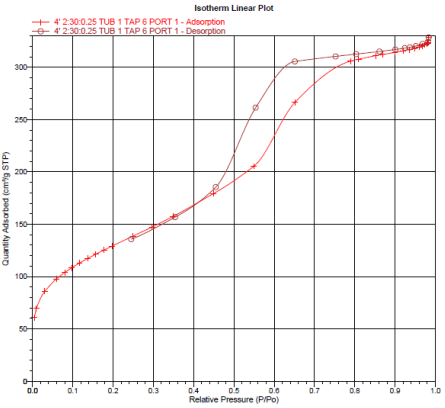

Figure 38. Isotherm of Experiment 4 (2:30:0.25)

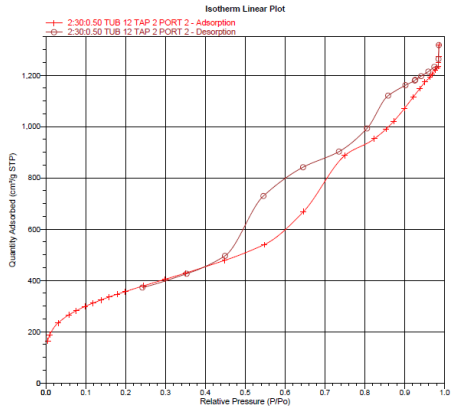

Figure 39. Isotherm of Experiment 5 (2:30:0.50)

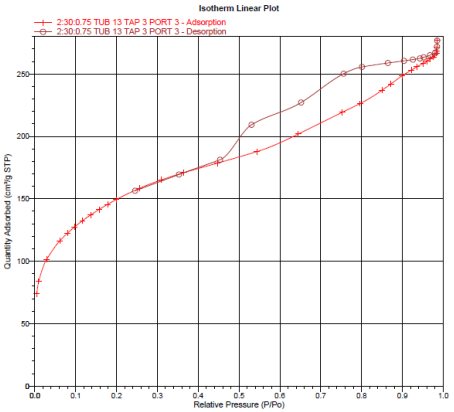

Figure 40. Isotherm of Experiment 6 (2:30:0.75)

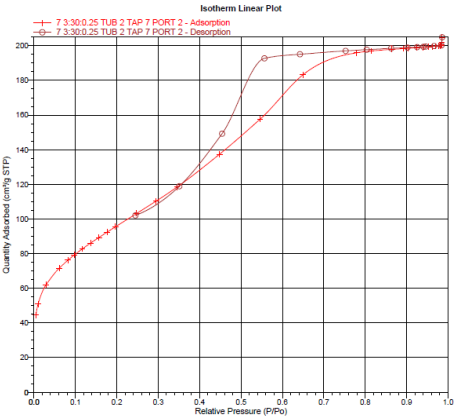

Figure 41. Isotherm of Experiment 7 (3:30:0.25)

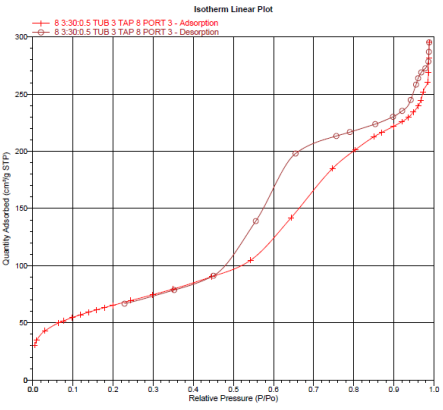

Figure 42. Isotherm of Experiment 8 (3:30:0.50)

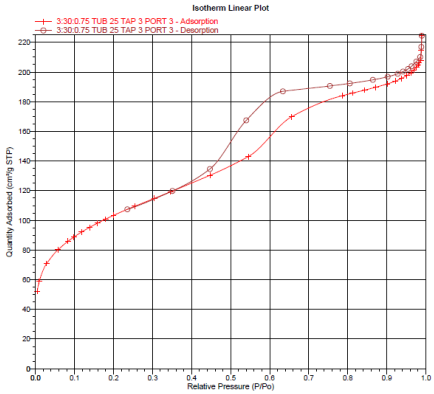

Figure 43. Isotherm of Experiment 9 (3:30:0.75)

APPENDIX 3: TEM IMAGES

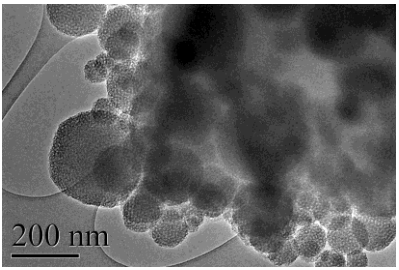

Figure 44. Experiment 1 (1:30:0.25).

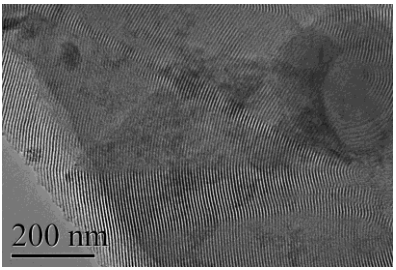

Figure 45. Experiment 5 (2:30:0.50).

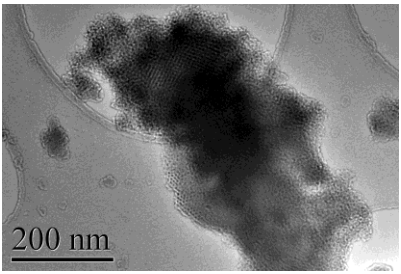

Figure 46. Experiment 6 (2:30:0.75).

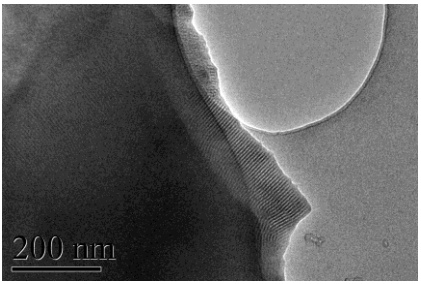

Figure 47. Experiment 7 (3:30:0.25).